The influence of training sample size on the accuracy of deep learning models for the prediction of soil properties with NIR spectroscopy data

Wartini Ng[1], Budiman Minasny[1], Wanderson de Sousa Mendes[2], José A.M.Demattê [2],

[1] School of Life and Environmental Sciences & Sydney Institute of Agriculture, The University of Sydney, NSW, Australia

[2] Department of Soil Science, "Luiz de Queiroz" College of Agriculture, University of São Paulo, Av. Pádua Dias 11, Portal Box 9, Piracicaba, São Paulo state Code 13418-900, Brazil

Correspondence to: Wartini Ng (wartini.ng@sydney.edu.au)

Abstract

The number of samples used in the calibration dataset affects the quality of the generated predictive models using visible, near and shortwave infrared (VIS-NIR-SWIR) spectroscopy for soil attributes. Recently, the convolutional neural network (CNN) is regarded as a highly accurate model for predicting soil properties on a large database. However, it has not been ascertained yet how large the sample size should be for CNN model to be effective. This paper investigates the effect of training sample size on the accuracy of deep learning and machine learning models. It aims at providing an estimate of how much calibration samples are needed to improve the model performance of soil properties predictions with CNN as compared to conventional machine learning models. In addition, this paper also looks at a way to interpret the CNN models, which are commonly labelled as black box. It is hypothesized that the performance of machine learning models will increase with an increasing number of training samples, but it will plateau when it reached a certain number, while the performance of CNN will keep improving. The performances of two machine learning models (Partial least squares regression (PLSR) and Cubist) are compared against the CNN model. A VIS-NIR-SWIR spectra library from Brazil containing 4251 unique sites, with averages of 2-3 samples per depth (a total of 12,044 samples), was divided into calibration (3188 sites) and validation (1063 sites) sets. A subset of the calibration dataset was then created to represent smaller calibration dataset ranging from 125, 300, 500, 1000, 1500, 2000, 2500 and 2700 unique sites, or equivalent to sample size approximately 350, 840, 1400, 2800, 4200, 5600, 7000, and 7650. All three models (PLSR, Cubist, and CNN models) were generated for each sample size of the unique sites for the prediction of five different soil properties, i.e. cation exchange capacity, organic carbon, sand, silt and clay content. These calibration subset sampling processes and modelling were repeated ten times to provide a better representation of the model performances. Learning curves showed that the accuracy increased with an increasing number of training sample. At a lower number of

samples (<1000), PLSR and Cubist performed better than CNN. The performance of CNN outweighed the PLSR and Cubist model at a sample size of 1500 and 1800 respectively. It can be recommended that deep learning is most efficient for spectra modelling for sample size above 2000. The accuracy of the PLSR and Cubist model seems to reach a plateau above sample size of 4200 and 5000, respectively, while the accuracy of CNN has not plateaued. A sensitivity analysis of the CNN model demonstrated the ability to determine important wavelengths region that affected the predictions of various soil attributes.
Keywords: convolutional neural network, deep learning, machine learning, infrared spectroscopy, soil properties, soil analysis

1. Introduction

There has been an increasing demand for a rapid and cost-effective method as an alternative for conventional laboratory soil analysis. Visible, near and shortwave infrared (VIS-NIR-SWIR) spectroscopy has been proposed to be used as an alternative tool for soil analysis for the last few decades (Bendor and Banin, 1995;Shepherd and Walsh, 2002;Stenberg et al., 2010). This method enables the simultaneous prediction of various properties and has non-destructive characteristics.

Various machine learning models, such as Partial Least Squares Regression (PLSR), Cubist, random forest, and support vector machines had been utilized to model spectroscopy data. However, the performances of these regression models are dependent on the spectra pre-processing methods (Rinnan et al., 2009), as well as the size and representativeness of the calibration samples (Kuang and Mouazen, 2012;Ng et al., 2018). Different combinations of the spectra pre-processing methods will result in various model performances. Furthermore, the spectra pre-processing techniques developed for a particular dataset might not work for a different dataset. Better generalization can be made by training the model in a larger dataset. However, several studies demonstrated that the performance of the machine learning model did not increase significantly or even plateaued as the calibration sample size increased (Figueroa et al., 2012;Ramirez-Lopez et al., 2014;Ng et al., 2018).

Advances in artificial intelligence, such as deep learning enable the possibility of extracting features from data without hand-engineered features (LeCun et al., 2015), such as pre-processing. Various deep learning convolutional neural network (CNN) model (AlexNet, VGGnet, GoogLeNet, ResNet), had been developed and trained on large volumes of data, which included over 10 million image data (Krizhevsky et al., 2012;Simonyan and Zisserman, 2014;Szegedy et al., 2015;He et al., 2016). Although CNN often deals with images as input data, it has recently been successfully applied to vibrational and reflectance spectroscopy (Acquarelli et al., 2017;Cui and Fearn, 2018;Liu et al., 2018;Ng et al., 2019;Padarian et al., 2019;Tsakiridis et al., 2020). Acquarelli et al. (2017) found that the CNN based model outperformed other models (Partial Least Square – Least Discriminant Analysis, logistic regression and k-nearest neighbour) for the classification of various vibrational spectroscopy data. CNN also has recently been successfully utilized for regression modelling using reflectance spectroscopy data (Cui and Fearn, 2018;Liu et al., 2018;Ng et al., 2019;Padarian et al., 2019). Cui and Fearn (2018) compared the performance of CNN and PLSR to predict protein and ash content of wheat kernels and wheat flour from the NIR-SWIR spectra data with calibration sample size ranging from 415 – 6,987. Liu et al. (2018) developed one-dimensional CNN model using VIS-NIR-SWIR spectra data to predict clay content with a calibration sample size of 16,000. Other studies had shown that CNN model had the capability to outperform PLSR and Cubist model for the prediction of various soil properties using VIS-NIR-SWIR (Ng et al., 2019;Padarian et al., 2019), mid-infrared (MIR) and combined VIS-NIR-SWIR with MIR spectra (Ng et al., 2019) with a calibration sample size greater than 10,000.

Deep learning such as CNN was developed to handle a large amount of data (millions of images), and soil spectra libraries these days are not that large yet. For example, a recent study used deep learning on 135 soil samples (Chen et al., 2018). The

advantage of using CNN on such a small number of samples is uncertain. A recent review on spectroscopy showed that there were several studies where deep learning was used with a small calibration sample size (Yang et al., 2019). The review indicated that increase in calibration sample size should further improve the calibration performance. However, there was no guideline how much improvement can be expected and what was the minimum number of samples for it to be effective.

A strategy to select adequate calibration set in terms of representativeness and size is vital in obtaining a model with good generalization ability. Although various sampling algorithms (Kennard-Stone, conditioned Latin Hypercube sampling, k-means clustering) to select representative samples have been explored (Ramirez-Lopez et al., 2014;Ng et al., 2018), the question of how many samples are needed for the CNN model to perform better than machine learning models for spectroscopy data has yet to be determined. It is commonly depicted and hypothesized in a learning curve that as more data are available, CNN will outperform traditional machine learning models (Mahapatra, 2018) (see Figure 1). Machine learning models tend to reach a plateau or show marginal improvement with an increasing amount of data as the model has limited complexity to deal with an increasing amount of data (Zhu et al., 2016).

Thus, the purpose of this study is to assess the amount of calibration data needed for the CNN model to outperform machine learning models. PLSR and Cubist are chosen as the representatives of the machine learning models which had been found to perform well in soil spectra data (e.g., Dangal et al. (2019)). In addition, to be able to predict soil properties accurately, we need to understand and interpret how a CNN model can predict soil properties from spectra. This paper presents the following specific contributions:

- testing the idea that common machine learning models will reach a plateau in accuracy with an increasing number of calibration samples,
- establishing the number of calibration samples required for deep learning to be effective for VIS-NIR-SWIR spectra data,
- establishing how much improvement in accuracy is achieved when the number of calibration sample for deep learning and machine learning models is increased, and
- demonstrating how to interpret deep learning model using a sensitivity analysis.

2. Materials and Methods

2.1. Dataset and chemical analysis

This dataset comprises 12,044 soil samples from 4,251 unique sites. The soil samples, collected from several regions of Brazil, i.e., states of Sao Paulo, Minas Gerais, Goias, and Mato Grosso do Sul. This dataset is part of The Brazilian Soil Spectral Library and extracted from Terra et al. (2018) and Bellinaso et al. (2010). The soils were derived mostly from basalt (volcanic rock) and sedimentary rocks (sandstone). Each site has up to seven measurements from the surface up to 1 m depth.

The measured properties include soil texture (sand, silt, and clay), organic carbon (OC) and cation exchange capacity (CEC). The soil particle size was quantified by the pipette method, as described in Donagema et al. (2011). The method consists of using a 0.1 M NaOH solution as dispersing agent under high-speed mechanical stirring during 10 min. Then, the sand fraction was separated by sieving and the clay portion by sedimentation. The silt was quantified based on pre- and post-difference. Organic carbon (OC) was determined by the Walkley and Black method (Walkley and Black, 1934), in which OC was oxidised using $K_2Cr_2O_7$ in a wet environment and then measured by titration with 0.1 M ammonium iron sulphate. As described in Donagemma et al. (2011), a 1 M KCl solution was used to extract aluminium, exchangeable calcium and magnesium. The atomic absorption spectrophotometry was used to quantify Ca and Mg concentrations. Aluminium concentration was determined by titrating with 0.025 M NaOH. Potassium and phosphorus contents were extracted using Mehlich-1 (0.05 M HCl with 0.0125 M H_2SO_4) solution. The concentration of P was quantified by colourimetry and the K concentration by flame photometry. Afterwards, CEC was determined as the sum of exchangeable cations. The descriptive statistics of the soil properties measured are included in Table 1.

2.2. Spectra measurements

The VIS-NIR-SWIR spectra of the soil samples were obtained with FieldSpec3 spectroradiometer (Analytical Spectral Devices, Boulder, Colorado) with a spectra range of visible to shortwave infrared (350 – 2500 nm) and spectra resolution of 1 nm from 350 to 700 nm, 3 nm from 700 to 1400 nm, and 10 nm from 1400 to 2500 nm. The sensor scanned an area of approximately 2 cm^2, and a light source was provided by two external 50-W halogen lamps. These lamps were positioned at a distance of 35 cm from the sample (non-collimated rays and a zenithal angle of 30°) with an angle of 90° between them. A Spectralon (Labsphere Inc., North Sutton, NH) standard white plate was scanned every 20 min during calibration. The samples were oven-dried at 45°C for 48 hours before being ground and sieved ≤ 2 mm. The sample was distributed homogeneously in Petri dishes for spectra measurement. Three replicates (involving a 180° turn of the Petri dish) were obtained for each sample. Each spectrum was averaged from 100 readings over 10 s.

2.3. Training and validation

To better represent the soil distribution, we split and subset the data based on sites. The dataset is first randomly split into 75% calibration (3188 sites) and 25% validation (1063 sites) based on the unique sites.

From the calibration dataset, smaller sample sizes ranging from 125, 300, 500, 1000, 1500, 2000, 2500 and 2700 unique sites were created, which is equivalent to a sample size of approximately 350, 840, 1400, 2800, 4200, 5600, 7000, and 7650. Better representations of model performances were provided by ten replicates of these sizes. Each sampling for the same number of sites could generate a slightly different number of samples since the number of measurements varied from one site to another. However, the model performance was evaluated on the common validation dataset using a total of 1063 sites (sample size N

= 3017). Thus, we create a learning curve of the accuracy of the models of the validation dataset as a function of the number of calibration samples.

2.4. Chemometrics model

Prior to the development of machine learning models (PLSR and Cubist), the spectra data were subjected to some pre-processing methods: (i) conversion to absorbance followed by (ii) Savitzky - Golay smoothing filter with window size of 11 and second-order polynomial (Savitzky and Golay, 1964), (iii) spectra trimming to discard region that has low signal to noise ratio (<500 nm and between 2450 – 2500 nm) and (iv) standard-normal-variate (SNV) transformation (Barnes et al., 1989). For the CNN model, the spectra were only normalized with SNV before being fed into the model. Our previous research (Ng et al., 2019) found that CNN has its own filtering algorithm that made pre-processing not necessary. This filtering approach will be discussed in the results section.

2.4.1. PLSR model

PLSR is one of the standard and most commonly used models with the spectroscopy data. It is a linear chemometric regression model that projects spectra data into latent variables that explain the variances within the spectra data and the response variables (Wold et al., 1983). The optimal number of latent variables used in the PLSR regression that resulted in the smallest root mean square error (RMSE) using the cross-validation approach was used to create the models. PLSR was implemented in the R statistical software (R Core Team, 2020) using the “pls” package (Mevik et al., 2018).

2.4.2. Cubist model

Cubist is a rule-based data mining model, which is an extension of the M5 model tree by Quinlan (1993). Cubist has been used successfully in soil spectroscopy studies and in many cases found to perform better than PLSR and other machine learning models (Dangal et al., 2019). Cubist creates one or more rules, in which if the rules are met, a certain linear model can be utilized to predict the target task. The model was evaluated using the "Cubist" package (Kuhn and Quinlan, 2018) in R.

2.4.3. CNN model

The CNN model is composed of three types of layers: convolutional, pooling and fully-connected layer. The convolutional layer extracts feature from the inputs, the pooling layer reduces the dimensionality of the input feature, and the fully connected layer connects the outputs from previous layers to the desired target outputs. The CNN model utilized in this study was derived from our previous study (Ng et al., 2019), where the spectra data were fed into the model as one-dimensional data. The architecture of the CNN model is included in Table 2 and Figure 2. Some of the layers within the network are shared to enable simultaneous output predictions.

The CNN model was trained with an initial learning rate of 0.001 and Adam optimizer (Kingma and Ba, 2014). The network was trained using a batch size of 50, and a maximum epoch of 200. For model optimization purposes, the calibration data is further divided into 75% train and 25% test set. Dropout, early stopping and reduced learning rates are used as a regularization technique to prevent network overfitting. For further details of the CNN model, the reader is referred to Ng et al. (2019). The CNN model was implemented in Python (v3.5.1; Python Software Foundation, 2017) using Keras library (v2.1.2; Chollet, 2015) and Tensorflow (v1.4.1; Abadi et al., 2015) backend.

All the model performances are compared in terms of coefficient of determination (R^2), and the root mean square error (RMSE), bias and ratio of performance to inter-quartile distance (RPIQ) values based on the validation dataset. Generally, larger values of R^2 and RPIQ and smaller bias and RMSE indicate better model performance.

2.5. Sensitivity analysis: evaluating important wavelengths

To uncover how CNN predicts different soil properties, a sensitivity analysis was conducted to assess the importance of each wavelength in contributing to predictions. Evaluating the sensitivity of the model can be done in several ways, for example, Cui and Fearn (2018) calculated the sensitivity of a CNN model for NIR by taking a numerical partial derivative of the output with respect to each wavelength. For wavelength *i*, the sensitivity *S* was calculated as:

$$S_i = \frac{f(\boldsymbol{X}_1, \dots, \boldsymbol{X}_i + \varepsilon, \dots, \boldsymbol{X}_n) - f(\boldsymbol{X})}{\varepsilon} \quad \text{(Eq. 1)}$$

where $\boldsymbol{X}$ is the reflectance spectra, and $f(\boldsymbol{X})$ is the CNN prediction using the spectra, ε is a small number. The idea is that if wavelength *i* has an important contribution to the prediction, a small perturbation to the reflectance value will create a large change in the prediction.

In our previous study (Ng et al., 2019), we calculated the sensitivity as a function of the variance of the model for each window of spectra. Here, we calculate the sensitivity based on the variance principle as an alternative approach:

$$S_i = \frac{Var\,(f(\boldsymbol{X}_1, \dots, \boldsymbol{X}_i, \dots, \boldsymbol{X}_n) - f(\overline{\boldsymbol{X}}))}{Var\,(\boldsymbol{Y})} \quad \text{(Eq. 2)}$$

Where Var is the variation calculation, $f(\boldsymbol{X}_1, \dots, \boldsymbol{X}_i, \dots, \boldsymbol{X}_n)$ is the prediction of spectra due to variation in wavelength i with other wavelengths held constant at their mean values, and $f(\overline{\boldsymbol{X}})$ is the prediction value using the mean values of the spectra and $\boldsymbol{Y}$ is the observed values of the target variable. In essence, we calculated how the model varied in comparison to the observations as a function of wavelength.

The current sensitivity analysis (Eq. 2) considers the actual variance of the data for a better approximation of wavelengths sensitivity. To calculate the variance sensitivity, two new data frames are created. The first data frame contains data which is the average of all the validation spectra data ($\bar{\boldsymbol{X}}$) and the second contains modified average spectra data ($\bar{\boldsymbol{X}}_i$), in which some of the average measurements are replaced with the actual spectra reflectance at a wavelength width of 5 nm.

The illustrations of the process of deriving new data frames are included in Figure 3. Both data frames are then fed into the pre-trained CNN model ($f()$). The variance between the average and modified average spectra are then compared to the actual variance of the target properties as a measure of the model sensitivity (Eq. 2).

3. Results

3.1. VIS-NIR-SWIR spectra characteristics

Large variability within the soil properties and texture could potentially influence the soil spectra characteristics (shown in Figure 4). In general, there was an increase in reflectance between 400 - 1000 nm, with several prominent absorption features at 1400, 1900 and 2200nm. Absorption features in the VIS-NIR (400 - 1000 nm) which is related to iron oxides, such as haematite (Fe_2O_3) and goethite (FeOOH) (Clark, 1999). Absorption near 1400 nm is associated with the first overtone of an O-H stretch vibration of water or metal-O-H vibration, while absorption is 1900 nm is combination vibrations of water related to H-O-H bend and O-H stretch (Viscarra Rossel et al., 2009). Absorption in the 2100-2400 nm region is related to the combination vibrations of minerals. Generally, spectra that have a higher clay content would show smaller reflectance (greater absorption) values in comparison to those with lower clay content. The representative samples of the VIS-NIR-SWIR spectra before and after pre-processing were included in Figure 4.

3.2. Visualization of the spectra within CNN model

An attempt to take a look at what the CNN model actually learns was conducted. As the raw reflectance spectrum was fed into the CNN model, it passed through a convolutional layer which extracted information from the spectra. Filters from the first two convolutional layers were included in Figure 5. Though only raw spectra were fed into the CNN model, we could see that the spectra underwent some spectra pre-processing within each filter of the layers. Some of the filters shown in the first convolution layer looked like the input spectra pattern (filter #3, 4 and 10), and some of them mimicked like transformation pattern: absorbance (filter #1, 5, 6, 7, 9, 13 and 16) and derivatives (filter # 2, 8, 11, 12, 14 and 15). The spectrum became smoother when they passed through the second convolutional layer, where some filters only accentuated certain peaks (Figure 5).

3.3. Prediction of soil properties and model comparison

The model performances for the validation dataset using the full calibration data (n_{site}= 3188, N=9027) for various soil properties and chemometrics model were presented in Table 3. CNN model outperformed both Cubist and PLSR model (in terms of higher R^2 and RPIQ and lower RMSE).

The performance achieved using the CNN model with the prediction of sand (R^2= 0.85; RPIQ =1.52), silt (R^2=0.58; RPIQ =0.75), clay (R^2=0.86; RPIQ =1.05), OC (R^2=0.69; RPIQ =0.91) and CEC (R^2=0.68; RPIQ =0.69). Both the PLSR and Cubist had similar performance for the prediction of the various properties. PLSR model achieved R^2 of 0.79, 0.47, 0.80, 0.48 and 0.52, and RPIQ of 1.29, 0.67, 0.87, 0.70, and 0.57 for the prediction of sand, silt, clay, OC, and CEC respectively. Meanwhile, Cubist model achieved R^2 of 0.78, 0.45, 0.81, 0.54 and 0.52 and RPIQ of 1.19, 0.67, 0.92, 0.70 and 0.59 for the prediction of sand, silt, clay, organic carbon, and CEC respectively. Nonetheless, on some cases, the CNN model prediction yielded higher bias on the prediction of some soil properties, such as OC and CEC (bias = -0.06 and -0.76 respectively), than PLSR model (bias = 0.02 and -0.17) for the same properties. The Cubist model yielded bias of -0.13 and -0.93 for the prediction of OC and CEC respectively.

Among all the properties predicted, the sand and clay content showed the best performance with R^2 values greater than 0.75 regardless of the types of model used ranging from (0.78 – 0.85 and 0.8 – 0.86) respectively. This finding is in agreement with the ones from Demattê et al. (2016), who observed good predictions for sand and clay content with R^2 of 0.86 and 0.85. Pinheiro et al. (2017) reported the prediction accuracy of 0.62 and 0.78 for the sand and clay content, respectively. The low performance of the silt predicted can be linked to error associated with the laboratory analysis method, where the silt content is derived from the difference of the soil mass after the sand and clay content are determined. The prediction for OC content in our study ranges from R^2 of 0.48 – 0.69. Shibusawa et al. (2001) reported R^2 of 0.65 for the prediction of OC using slightly different wavelength region (400-2400nm). Our prediction of CEC ranges from R^2 of 0.52 – 0.68. Chang et al. (2001) and Islam et al. (2003) reported R^2 of 0.81 and 0.88, respectively for the prediction of CEC. Although some prediction accuracies are slightly lower than other studies, they are still within an acceptable range.

3.4. Effect of sample training size: learning curve

A total of nine subset models based on the unique sample sizes were generated to investigate the effect of training sample size. The performance comparison of all the models expressed as average R^2 values is illustrated as a learning curve in Figure 6. The depicted R^2 values are the average performance prediction for all five properties of all ten replicates, except for the largest sample size (N = 9027) where a single data random split for validation of the data is used. The learning curve generally follows the common pattern found in machine learning studies (Figueroa et al., 2012), the performance increased rapidly with an increase in the size of the training set from around 350 to 1400. For PLSR and Cubist, the growth in performance became slower after it reached 2800 samples. PLSR performance reached a plateau after 4000 samples while the increase in performance in Cubist was marginal after 5500 samples.

In general, the PLSR and Cubist model tend to perform better when the sample size was relatively small (<1500). When the sample size was approximately 1800, there was only a small difference in the performances for all models. However, when the sample size was further increased (>2000), the CNN model started to show better performance in comparison to both PLSR and Cubist model. The effectiveness of PLSR and Cubist model reached a plateau at approximately 4000 and 5500 samples, respectively, while the performance of CNN was still increasing, as depicted in the theoretical curve (Figure 1). The slight drop in Cubist's performance at sample size 9027 was because there was only one realization of data split (75% of the data).

We further compared the average model performance based on the RMSE ratios of machine learning models against the CNN model (Figure 7). This comparison was developed using the model performance for each unique property, and the variances presented was based on ten simulations. If a particular model X performs better than the Y model it is compared against, the RMSE ratios of X/Y should be less than one.

Upon comparing the RMSE ratios of PLSR/Cubist model, we found that PLSR performed better than the Cubist model when the sample size is less than 1400. Cubist model performed better than the PLSR model as the sample size was increased. Using the RMSE ratios of PLSR/CNN model, PLSR was found to perform better than CNN when the sample is less than 1400 (Figure 7). Similar performance of both PLSR and CNN model was achieved when the sample size is approximately 1400. In terms of RMSE ratios of Cubist/CNN, overall CNN model performed better in comparison to the Cubist model regardless of sample size. This was slightly different than the one that was observed when only R^2 parameter was utilized. The RMSE ratios of Cubist/CNN seemed to vary more for a smaller sample size (longer whisker). When the sample size is approximately 850, both models seemed to perform similarly. A portion of the model performed better, while the remaining performed worse. As the calibration sample size increased, the CNN model performed better in comparison to the Cubist model. Thus, it can be recommended that the current CNN model structure is most efficient for VIS-NIR-SWIR spectra modelling with sample size above 2000. CNN still can be used for small number of samples, but its performance is not better than PLSR or Cubist.

3.5. Sensitivity Analysis

The critique of CNN is that it is a complex model and a black box. To uncover how the CNN model works, a sensitivity analysis was conducted to show how CNN is predicting each of the soil properties, illustrated in Figure 8. Only certain parts of the spectra were used by the CNN model for prediction, which corresponded to the soil properties and composition. The important wavelengths for the prediction of CEC are between the regions of 1600 – 2000 nm. This result is similar to the observations made by Lee et al. (2009) on the surface horizon dataset where 1772 and 1805 nm are essential in predicting the CEC. The presence of high CEC is often linked to the presence of OC and clay content. It is interesting that the same region is important in predicting organic carbon but not clay content. Aside from the same region used by CEC, wavelengths' region between 1100 – 1200 nm are also deemed relevant by the CNN model for the prediction of OC content. This finding is slightly

different to those reported by Lee et al. (2009) in which the important wavelengths reported are at 1772, 1871, 2069, 2246, 2351 and 2483 nm for the profile dataset and 1871, 2072 and 2177 nm for the surface horizon dataset.

Similar wavelength regions are deemed to be important in predicting the soil texture although the importance slightly varied among the type of texture of interest (sand, silt and clay) at wavelengths between 500 and 1800 nm. The important wavelengths for the prediction of sand and clay content share a higher similarity in comparison to that of silt content prediction. The most crucial wavelength identified is around 850 nm for the prediction of sand and clay content, and around 1100 nm for the prediction of silt content. These observations are also different from those reported by Demattê (2002) and Lee et al. (2009) where the important wavelengths for the prediction of soil texture are at 1800 – 2400 nm. In particular, the soil texture prediction found in the CNN model is strongly related to hematite and/or goethite, -OH and Al-OH groups from kaolinite (Viscarra Rossel and Behrens, 2010;Pinheiro et al., 2017;Fang et al., 2018).

We also compare important wavelengths from the machine learning models against the one from the deep learning model for the prediction of OC as an example. Common wavelengths found to be related to the organic carbon predictions are 1100, 1600, 1700 – 1800, 2000, 2200 – 2400 nm (Dalal and Henry, 1986;Stenberg et al., 2010).

As a comparison, we calculated important wavelengths used in the PLSR and Cubist models. The important wavelengths utilized in the PLSR model was derived based on the absolute value of the regression coefficients. The height of the line indicates the importance of particular wavelengths for the determination of organic carbon content in the soil. Important wavelengths identified for the prediction of organic carbon were 500 – 700, 1400 and 1715 nm.

The wavelengths used in the Cubist were derived based on model usage either as predictors (blue lines) or conditions (pink lines) (Figure 9). Some of the wavelengths used in the Cubist model are similar to those observed in the PLSR model, in particular the visible (500 – 700 nm), and shortwave infrared regions (1400 and 1900 nm).

4. Discussion

4.1. Understanding the CNN models

While conventional PLSR and machine learning models require spectra pre-processing for the spectra data input, CNN model takes raw spectra as inputs. CNN has been shown to be a successful end-to-end learning model which learn feature automatically while minimizing hand-crafted pre-processing process. Upon taking a closer look at the various filters within the convolutional layers, we found that the filters behaved like spectra pre-processing method. It is interesting to note that using the raw spectra input, various spectra pre-processing that was commonly used within spectroscopy could be observed within the layer itself. Given the various complexity within the CNN model, the use of spectra pre-processing prior to being

fed is unnecessary. This advantage opens up possibilities of developing highly accurate chemometrics model, which also plays a role in automatic spectra pre-processing.

CNN have been proven to be extremely successful, however how they work remains largely a mystery as they are buried in layers of computations. Sensitivity analysis enabled us to see better the inner workings of the CNN model. We could understand better which wavelengths features are essential from the spectra when used in developing the regression prediction. Important wavelengths derived from the sensitivity analysis based on the CNN model looked slightly different from those of PLSR and Cubist models. Wavelengths around the 1700 nm region were deemed to be the most important, followed by those between the 1150 nm region. Nonetheless, some of the important regions overlapped. It was also worth noting that the model did not use the visible part of the spectra for prediction. In comparison to the sensitivity of MIR spectra data on previous study (Ng et al., 2019), the NIR model's sensitivity index was much broader, which reflected NIR's characteristic broad peak.

Although all three methods used different ways to derive important wavelengths, PLSR model tended to use most parts of the spectra. When irrelevant wavelengths are included in model development, it may reduce the model performance. The Cubist model seemed more selective in terms of wavelengths used, however this example showed that it also used most parts of the VIS-NIR-SWIR spectra. CNN model used wavelengths between 800 – 2000 nm, with emphasis around 1100 and 1700 nm.

4.2. The effect of calibration sample size to model performance

PLSR, Cubist and CNN represent models with increased complexity. By combining results from 5 soil properties, we can show better a generalisation of the performance of the models as a function of training sample size. Simpler models (PLSR) performed better at a smaller sample size (< 1400). Cubist outperformed PLSR at sample size > 2000, while CNN outweighed other models when sample size > 2500. The increase in the accuracy of machine learning models (PLSR and Cubist) became insignificant when the number of samples was greater than 5000. This trend of plateauing of performance (maximized up to a certain point) with an increase in sample size as had been observed by several authors (Shepherd and Walsh, 2002;Kuang and Mouazen, 2012;Ramirez-Lopez et al., 2014;Ng et al., 2018). This trend is related to the complexity of the model, as a simpler model (such as PLSR) cannot capture all variation in the data. Thus, a more complex model is suitable when the number of samples is large.

Previous studies by Ng et al. (2019) and Padarian et al. (2019) had shown that CNN performed better than PLSR and Cubist when the model was trained with more than 10,000 samples. However, there were also studies using CNN with a small number of training samples. This study showed that CNN model only outperformed PLSR and Cubist models when the sample size is greater than 2000. As sample size increases, the efficiency of CNN model is increased. We observed a larger reduction in RMSE (CNN compared to the other 2 models) with increasing calibration sample size. Thus, we recommend using a minimum

of 2000 samples to train CNN model for the VIS-NIR-SWIR spectra. To further improve the performance of the CNN model, simultaneous prediction of soil properties could also be implemented within the model.

The advantage of using deep learning on a small number of samples is minimal as CNN is a data-hungry model; it is also more computationally expensive than the typical machine learning models. While our results pertain to the spectra dataset from Brazil and a particular structure of the CNN, we believe our results can serve as a guide on the number of samples needed to create a better deep learning model. Future research could test this idea on larger and more variable datasets (e.g. a global spectra library with more than 100,000 samples) and to see if a more complex and deeper network of CNN can handle such dataset.

5. Conclusions

We assessed the effect of training sample size and identified important wavelengths in predicting various soil properties using Cubist and CNN model. In general, the CNN model performed better than the Cubist when the sample size is relatively large (>2000). Here, we found that with its current model structure, CNN is more accurate than a machine learning model when the number of calibration samples is above 2000. The more complex and deeper network of a deep learning model, the more likely it will need a larger number of samples for training. PLSR and Cubist models perform less accurate than the CNN model as sample size increases, and both models reached a plateau after a sample size of 4000 – 5000. Meanwhile, the performance of CNN still increases until the maximum number of data used in this study (N = 9000). Future studies should explore larger dataset to see the generalization of the accuracy vs sample size and to explore if the deep learning CNN model ever reaches a plateau in accuracy.

Author contributions

Wartini Ng was responsible for the data analysis, and prepared the manuscript; Budiman Minasny contributed to the idea, data analysis and editing the manuscript; Wanderson de Sousa Mendes and José A.M.Demattê contributed to the idea, provided the data and editing the manuscript.

Competing interests

The authors declare that they have no conflict of interest.

Acknowledgements

This study was supported in part by the ARC Linkage Project LP150100566 - Optimised field delineation of contaminated soils. The authors would also like to thank members of the Geotechnologies in Soil Science Group (https://esalqgeocis.wixsite.com/geocis) and Sao Paulo Research Foundation (FAPESP, grant numbers 2014/22262-0 and 2016/26124-6). BM is a member of the GLADSOILMAP consortium supported by LE STUDIUM Loire Valley Institute for Advanced Studies through its LE STUDIUM Research Consortium Programme.

References

Acquarelli, J., van Laarhoven, T., Gerretzen, J., Tran, T. N., Buydens, L. M. C., and Marchiori, E.: Convolutional neural networks for vibrational spectroscopic data analysis, Anal Chim Acta, 954, 22-31, 10.1016/j.aca.2016.12.010, 2017.

Barnes, R. J., Dhanoa, M. S., and Lister, S. J.: Standard Normal Variate Transformation and De-Trending of near-Infrared Diffuse Reflectance Spectra, Appl Spectrosc, 43, 772-777, Doi 10.1366/0003702894202201, 1989.

Bellinaso, H., Demattê, J. A. M., and Romeiro, S. A.: Soil Spectral Library and Its Use in Soil Classification, Rev Bras Cienc Solo, 34, 861-870, Doi 10.1590/S0100-06832010000300027, 2010.

Bendor, E., and Banin, A.: Near-Infrared Analysis as a Rapid Method to Simultaneously Evaluate Several Soil Properties, Soil Sci Soc Am J, 59, 364-372, DOI 10.2136/sssaj1995.03615995005900020014x, 1995.

Chang, C. W., Laird, D. A., Mausbach, M. J., and Hurburgh, C. R.: Near-infrared reflectance spectroscopy-principal components regression analyses of soil properties, Soil Sci Soc Am J, 65, 480-490, 2001.

Chen, H. Z., Liu, Z. Y., Gu, J., Ai, W., Wen, J. B., and Cai, K.: Quantitative analysis of soil nutrition based on FT-NIR spectroscopy integrated with BP neural deep learning, Anal Methods-Uk, 10, 5004-5013, 10.1039/c8ay01076e, 2018.

Clark, R. N.: Chapter 1: Spectroscopy of Rocks and Minerals, and Principles of Spectroscopy, in: Manual of Remote Sensing, edited by: Rencz, A. N., Remote Sensing for the Earth Sciences, John Wiley and Sons, New York, 3- 58, 1999.

Cui, C. H., and Fearn, T.: Modern practical convolutional neural networks for multivariate regression: Applications to NIR calibration, Chemometr Intell Lab, 182, 9-20, 10.1016/j.chemolab.2018.07.008, 2018.

Dalal, R. C., and Henry, R. J.: Simultaneous Determination of Moisture, Organic-Carbon, and Total Nitrogen by near-Infrared Reflectance Spectrophotometry, Soil Sci Soc Am J, 50, 120-123, DOI 10.2136/sssaj1986.03615995005000010023x, 1986.

Dangal, S., Sanderman, J., Wills, S., and Ramirez-Lopez, L.: Accurate and Precise Prediction of Soil Properties from a Large Mid-Infrared Spectral Library, Soil Systems, 3, 11, https://doi.org/10.3390/soilsystems3010011, 2019.

Demattê, J. A. M.: Characterization and discrimination of soils by their reflected electromagnetic energy, Pesqui Agropecu Bras, 37, 1445-1458, Doi 10.1590/S0100-204x2002001000013, 2002.

Demattê, J. A. M., Bellinaso, H., Araujo, S. R., Rizzo, R., and Souza, A. B.: Spectral regionalization of tropical soils in the estimation of soil attributes, Rev Cienc Agron, 47, 589-598, 2016.

Donagema, G. K., de Campos, D. B., Calderano, S. B., Teixeira, W., and Viana, J. M.: Manual de métodos de análise de solo, Embrapa Solos-Documentos (INFOTECA-E), 2011.

Fang, Q., Hanlie, H., Zhao, L., Kukolich, S., Yin, K., and Wang, C.: Visible and near-infrared reflectance spectroscopy for investigating soil mineralogy, 2018.

Figueroa, R. L., Zeng-Treitler, Q., Kandula, S., and Ngo, L. H.: Predicting sample size required for classification performance, BMC Medical Informatics and Decision Making, 12, 8, 10.1186/1472-6947-12-8, 2012.

He, K. M., Zhang, X. Y., Ren, S. Q., and Sun, J.: Deep Residual Learning for Image Recognition, 2016 Ieee Conference on Computer Vision and Pattern Recognition (Cvpr), 770-778, 10.1109/Cvpr.2016.90, 2016.

Islam, K., Singh, B., and McBratney, A.: Simultaneous estimation of several soil properties by ultra-violet, visible, and near-infrared reflectance spectroscopy, Aust J Soil Res, 41, 1101-1114, 10.1071/Sr02137, 2003.

Kingma, D. P., and Ba, J.: Adam: A method for stochastic optimization, arXiv preprint arXiv:1412.6980, 2014.

Krizhevsky, A., Sutskever, I., and Hinton, G. E.: ImageNet classification with deep convolutional neural networks, Proceedings of the 25th International Conference on Neural Information Processing Systems - Volume 1, Lake Tahoe, Nevada, 2012.
Kuang, B., and Mouazen, A. M.: Influence of the number of samples on prediction error of visible and near infrared spectroscopy of selected soil properties at the farm scale, Eur J Soil Sci, 63, 421-429, 10.1111/j.1365-2389.2012.01456.x, 2012.
LeCun, Y., Bengio, Y., and Hinton, G.: Deep learning, Nature, 521, 436-444, 10.1038/nature14539, 2015.
Lee, K. S., Lee, D. H., Sudduth, K. A., Chung, S. O., Kitchen, N. R., and Drummond, S. T.: Wavelength Identification and Diffuse Reflectance Estimation for Surface and Profile Soil Properties, T Asabe, 52, 683-695, 2009.
Liu, L., Ji, M., and Buchroithner, M.: Transfer Learning for Soil Spectroscopy Based on Convolutional Neural Networks and Its Application in Soil Clay Content Mapping Using Hyperspectral Imagery, Sensors-Basel, 2018.
Why Deep Learning over Traditional Machine Learning?: https://towardsdatascience.com/why-deep-learning-is-needed-over-traditional-machine-learning-1b6a99177063, 2018.
Ng, W., Minasny, B., Malone, B., and Filippi, P.: In search of an optimum sampling algorithm for prediction of soil properties from infrared spectra, Peerj, 6, 10.7717/peerj.5722, 2018.
Ng, W., Minasny, B., Montazerolghaem, M., Padarian, J., Ferguson, R., Bailey, S., and McBratney, A. B.: Convolutional neural network for simultaneous prediction of several soil properties using visible/near-infrared, mid-infrared, and their combined spectra, Geoderma, 352, 251-267, https://doi.org/10.1016/j.geoderma.2019.06.016, 2019.
Padarian, J., Minasny, B., and McBratney, A. B.: Using deep learning to predict soil properties from regional spectral data, Geoderma Regional, 16, e00198, https://doi.org/10.1016/j.geodrs.2018.e00198, 2019.
Pinheiro, E. F. M., Ceddia, M. B., Clingensmith, C. M., Grunwald, S., and Vasques, G. M.: Prediction of Soil Physical and Chemical Properties by Visible and Near-Infrared Diffuse Reflectance Spectroscopy in the Central Amazon, Remote Sens-Basel, 9, 10.3390/rs9040293, 2017.
Quinlan, J. R.: C4.5: Programs for Machine Learning, Morgan Kaufmann Publishers Inc., San Mateo, California, 1993.
Ramirez-Lopez, L., Schmidt, K., Behrens, T., van Wesemael, B., Dematte, J. A. M., and Scholten, T.: Sampling optimal calibration sets in soil infrared spectroscopy, Geoderma, 226, 140-150, 10.1016/j.geoderma.2014.02.002, 2014.
Rinnan, A., van den Berg, F., and Engelsen, S. B.: Review of the most common pre-processing techniques for near-infrared spectra, Trac-Trend Anal Chem, 28, 1201-1222, https://doi.org/10.1016/j.trac.2009.07.007, 2009.
Savitzky, A., and Golay, M. J. E.: Smoothing and Differentiation of Data by Simplified Least Squares Procedures, Anal Chem, 36, 1627-1639, 10.1021/ac60214a047, 1964.
Shepherd, K. D., and Walsh, M. G.: Development of Reflectance Spectral Libraries for Characterization of Soil Properties, Soil Sci Soc Am J, 66, 988-998, https://doi.org/10.2136/sssaj2002.9880, 2002.
Shibusawa, S., Imade Anom, S. W., Sato, S., Sasao, A., and Hirako, S.: Soil mapping using the real-time soil spectrophotometer. In: Grenier, G., Blackmore, S. (Eds.), ECPA, Third European Conference on Precision Agriculture. : Agro Montpellier, 1. Montpellier, France, pp. 497–508., 2001,
Simonyan, K., and Zisserman, A.: Very Deep Convolutional Networks for Large-Scale Image Recognition, CoRR, abs/1409.1556, 2014.
Stenberg, B., Viscarra Rossel, R. A., Mouazen, A. M., and Wetterlind, J.: Chapter Five - Visible and Near Infrared Spectroscopy in Soil Science, in: Adv Agron, edited by: Sparks, D. L., Academic Press, 163-215, 2010.
Szegedy, C., Liu, W., Jia, Y. Q., Sermanet, P., Reed, S., Anguelov, D., Erhan, D., Vanhoucke, V., and Rabinovich, A.: Going Deeper with Convolutions, Proc Cvpr Ieee, 1-9, 2015.
Terra, F. S., Dematte, J. A. M., and Rossel, R. A. V.: Proximal spectral sensing in pedological assessments: vis-NIR spectra for soil classification based on weathering and pedogenesis, Geoderma, 318, 123-136, 10.1016/j.geoderma.2017.10.053, 2018.
Tsakiridis, N. L., Keramaris, K. D., Theocharis, J. B., and Zalidis, G. C.: Simultaneous prediction of soil properties from VNIR-SWIR spectra using a localized multi-channel 1-D convolutional neural network, Geoderma, 367, ARTN 114208 10.1016/j.geoderma.2020.114208, 2020.
Viscarra Rossel, R. A., Cattle, S. R., Ortega, A., and Fouad, Y.: In situ measurements of soil colour, mineral composition and clay content by vis–NIR spectroscopy, Geoderma, 150, 253-266, https://doi.org/10.1016/j.geoderma.2009.01.025, 2009.
Viscarra Rossel, R. A., and Behrens, T.: Using data mining to model and interpret soil diffuse reflectance spectra, Geoderma, 158, 46-54, 10.1016/j.geoderma.2009.12.025, 2010.

Walkley, A., and Black, I. A.: An examination of the Degtjareff method for determining soil organic matter, and a proposed modification of the chromic acid titration method, Soil Sci, 37, 29-38, Doi 10.1097/00010694-193401000-00003, 1934.
Wold, S., Martens, H., and Wold, H.: The Multivariate Calibration-Problem in Chemistry Solved by the Pls Method, Lect Notes Math, 973, 286-293, 1983.
Yang, J., Xu, J. F., Zhang, X. L., Wu, C. Y., Lin, T., and Ying, Y. B.: Deep learning for vibrational spectral analysis: Recent progress and a practical guide, Anal Chim Acta, 1081, 6-17, 10.1016/j.aca.2019.06.012, 2019.
Zhu, X., Vondrick, C., Fowlkes, C. C., and Ramanan, D.: Do We Need More Training Data?, International Journal of Computer Vision, 119, 76-92, 10.1007/s11263-015-0812-2, 2016.

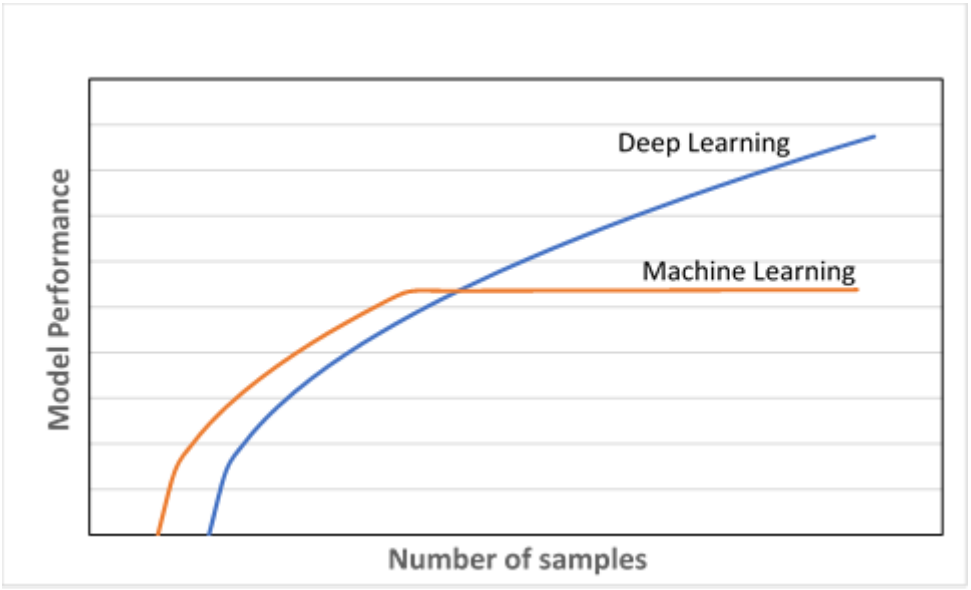

Figure 1. Model performance of deep learning vs other machine learning algorithms as a function of number of samples.

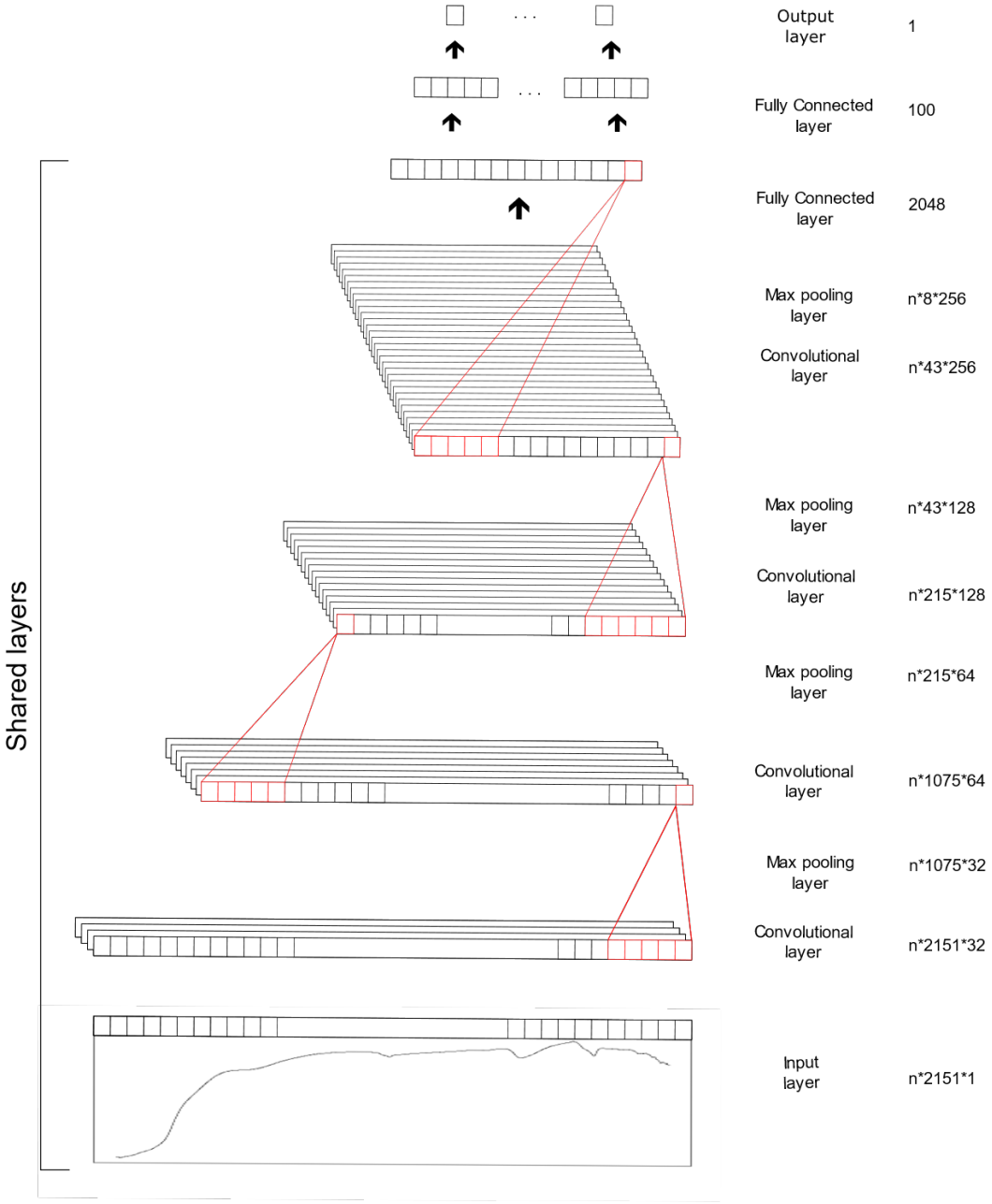

451

452 **Figure 2. Architecture of the one-dimensional Convolutional Neural Network (CNN) model.**

453

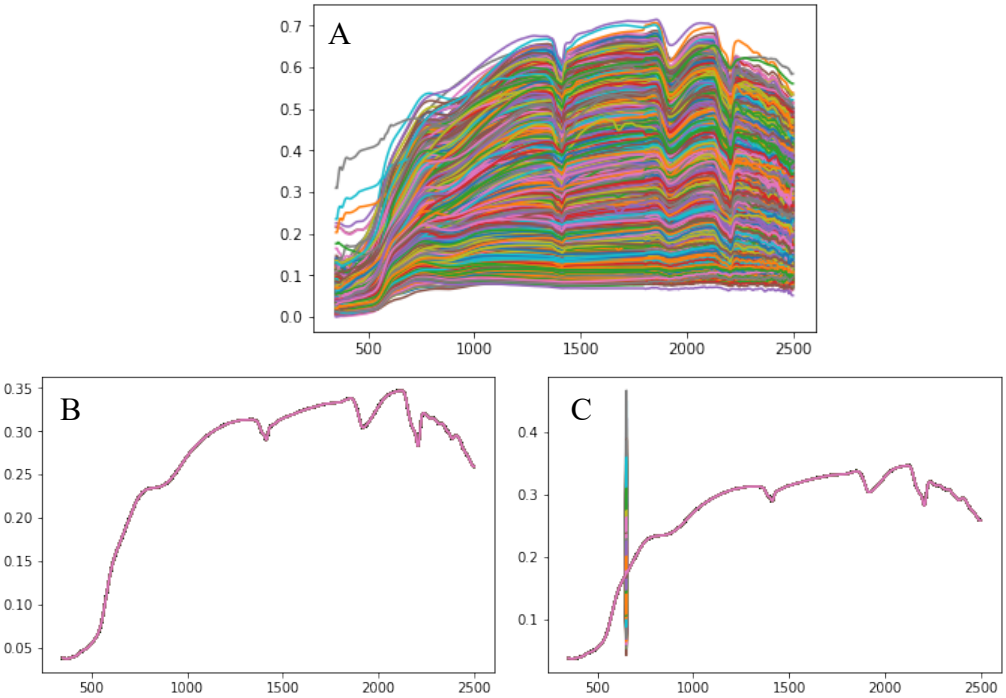

Figure 3. Illustration of sensitivity analysis process: (A) represents the validation spectra data, (B) represents the overall average of the validation spectra data and (C) represents the modified average of the validation spectra data.

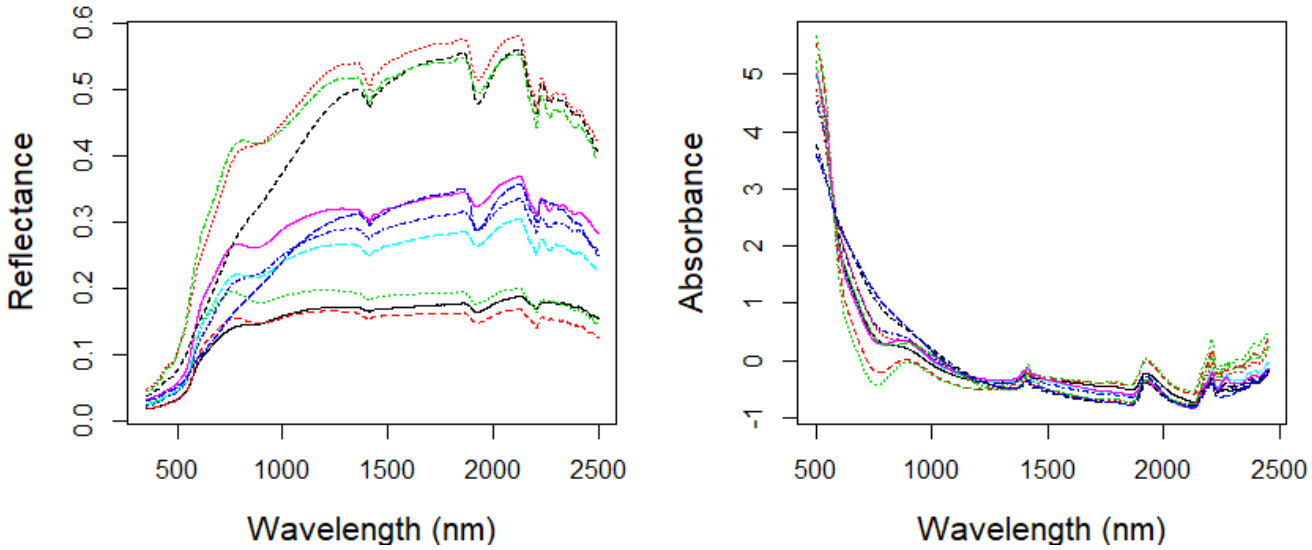

459

460 **Figure 4. Visible, near and shortwave infrared (VIS-NIR-SWIR) spectra of 10 soil samples without spectra pre-processing (left) and**
461 **with spectra pre-processing (right).**

462

Convolution #1: A few of the 32 filters

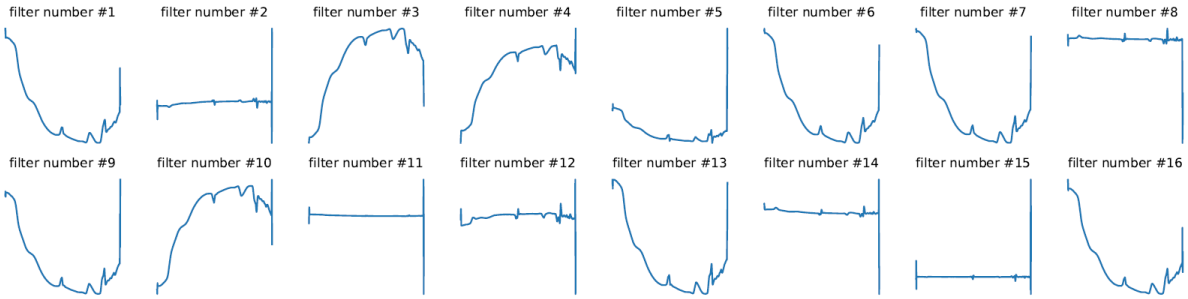

Convolution #2: A few of the 64 filters

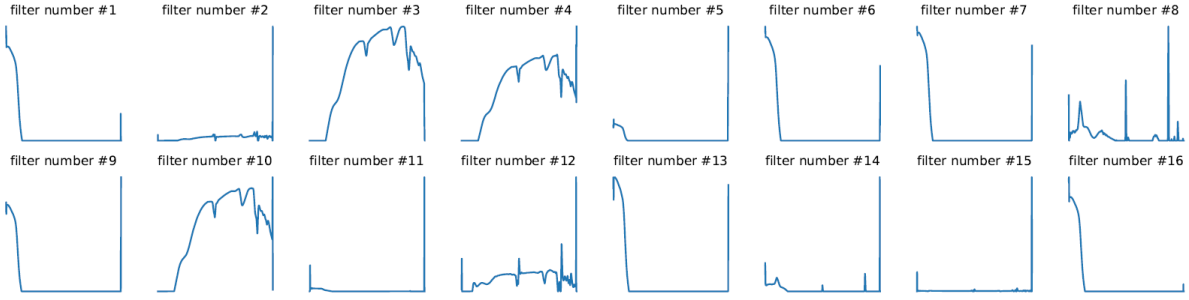

Figure 5. Visualization of the filters in the first two convolutional layers within the one-dimensional Convolutional Neural Network (CNN) model of the visible, near, and shortwave infrared (VIS-NIR-SWIR) spectra data.

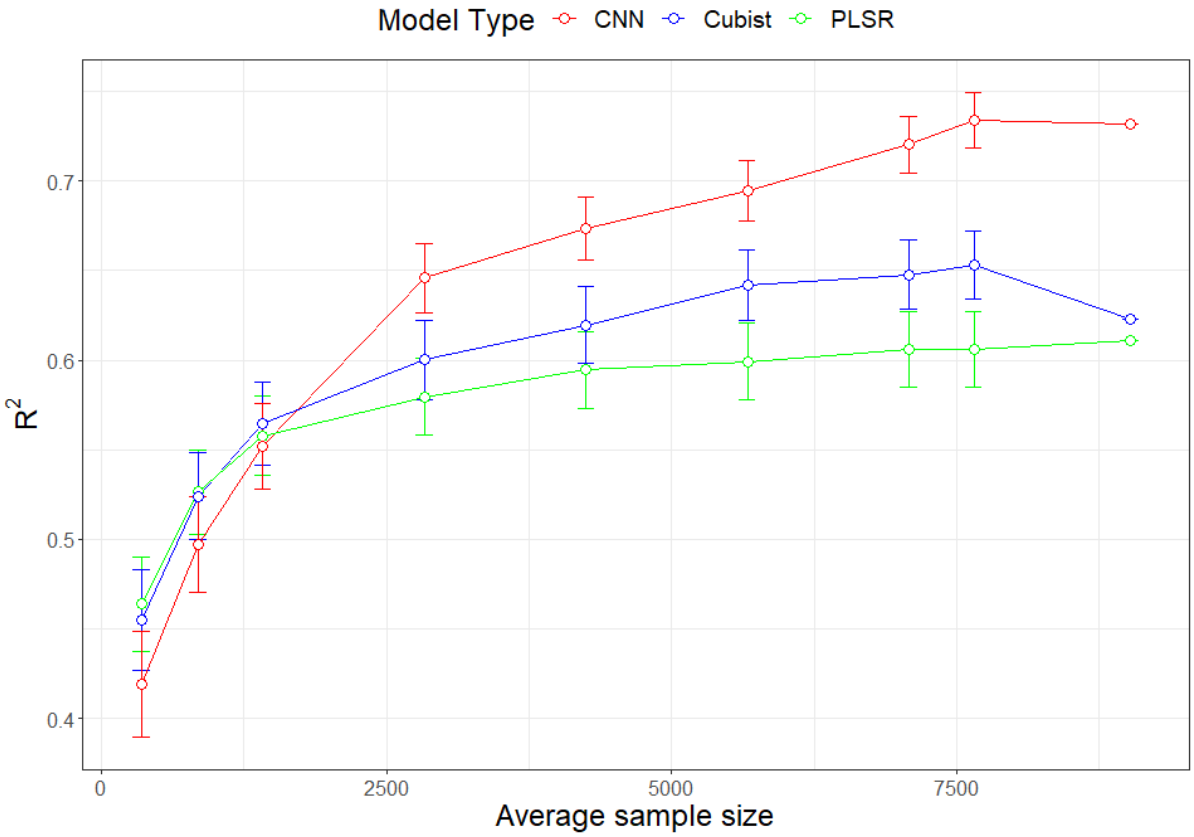

Figure 6. Model performances (in terms of average R^2 for five soil properties) as a function of sample size using Partial Least Squares Regression (PLSR), Cubist and Convolutional Neural Network (CNN) model based on ten simulations. The value for the largest sample size (N = 9027) is a single realization 75% of the data.

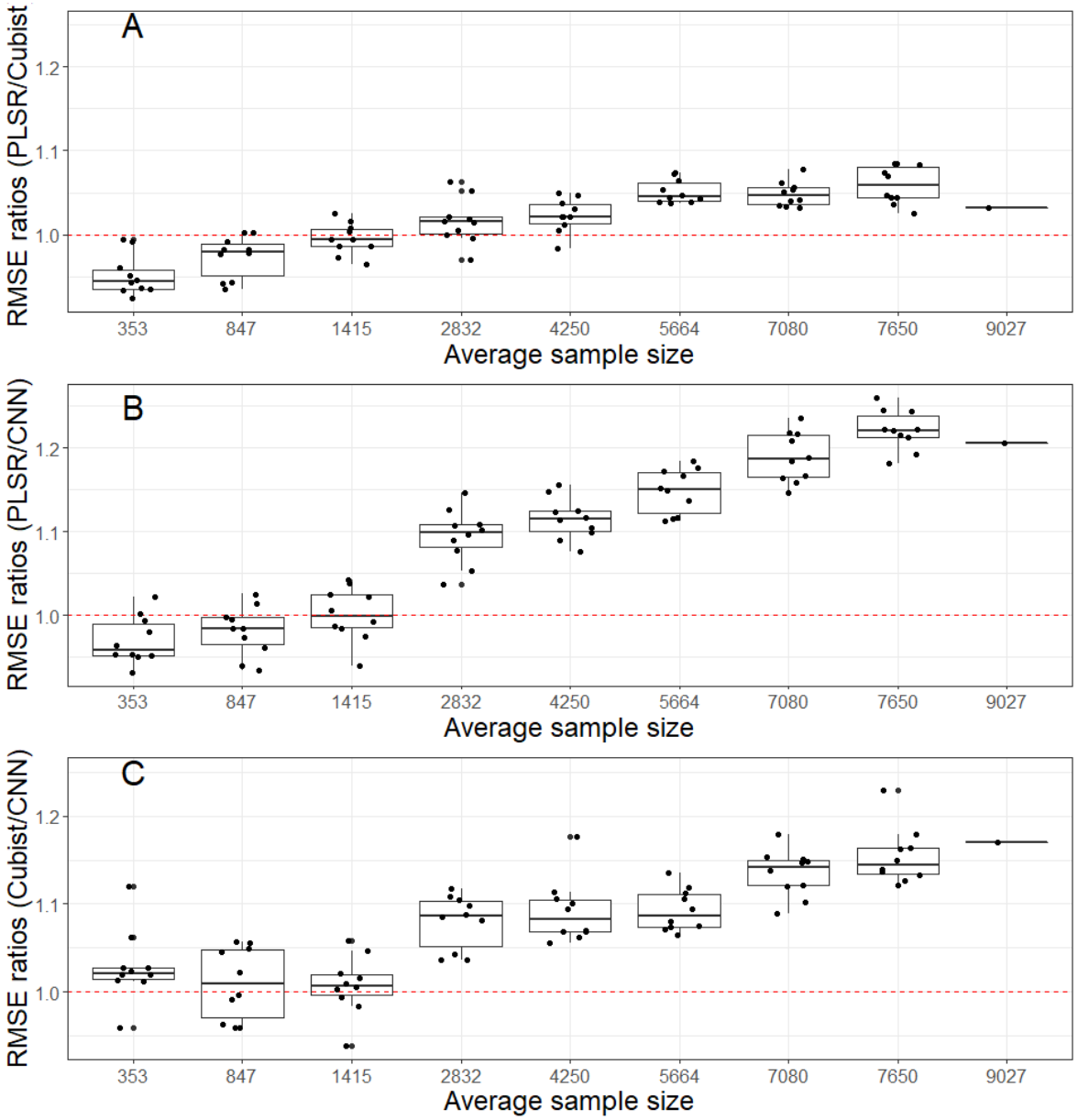

Figure 7. Model performances (in terms of root mean square error (RMSE) ratios of (A) Partial Least Squares Regression (PLSR) over Cubist model (B) PLSR over Convolutional Neural Network (CNN) model and (C) Cubist over CNN as an average of five soil properties) based on various sample size using ten simulations. The red – dotted line represents a 1:1 RMSE ratio.

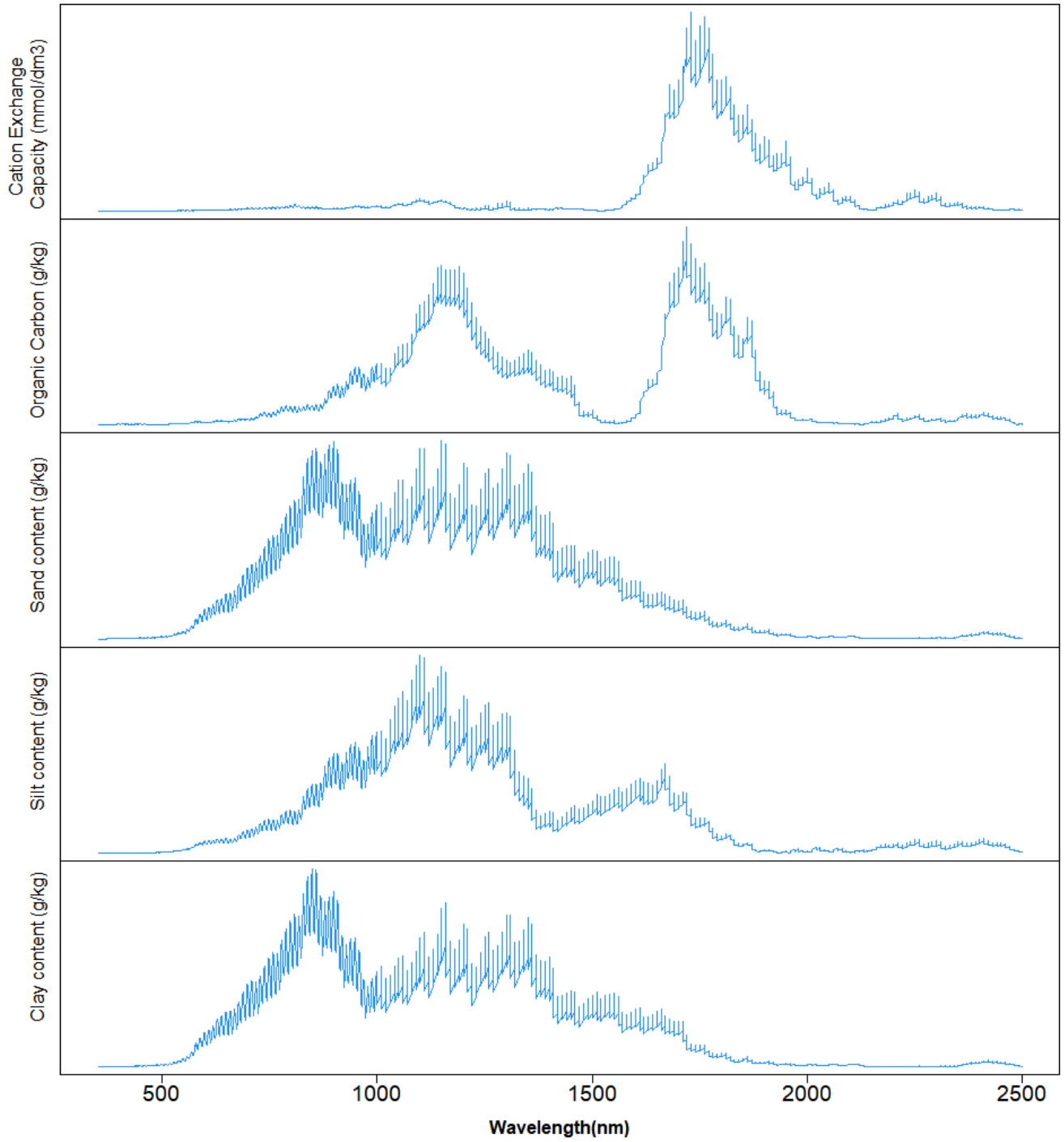

Figure 8: Sensitivity analysis of the visible, near and shortwave infrared (VIS-NIR-SWIR) spectra in predicting various soil properties using the Convolutional Neural Network (CNN) model. The graph depicts sensitivity index (calculated from(Eq. 2)) for different soil properties as a function of wavelength.

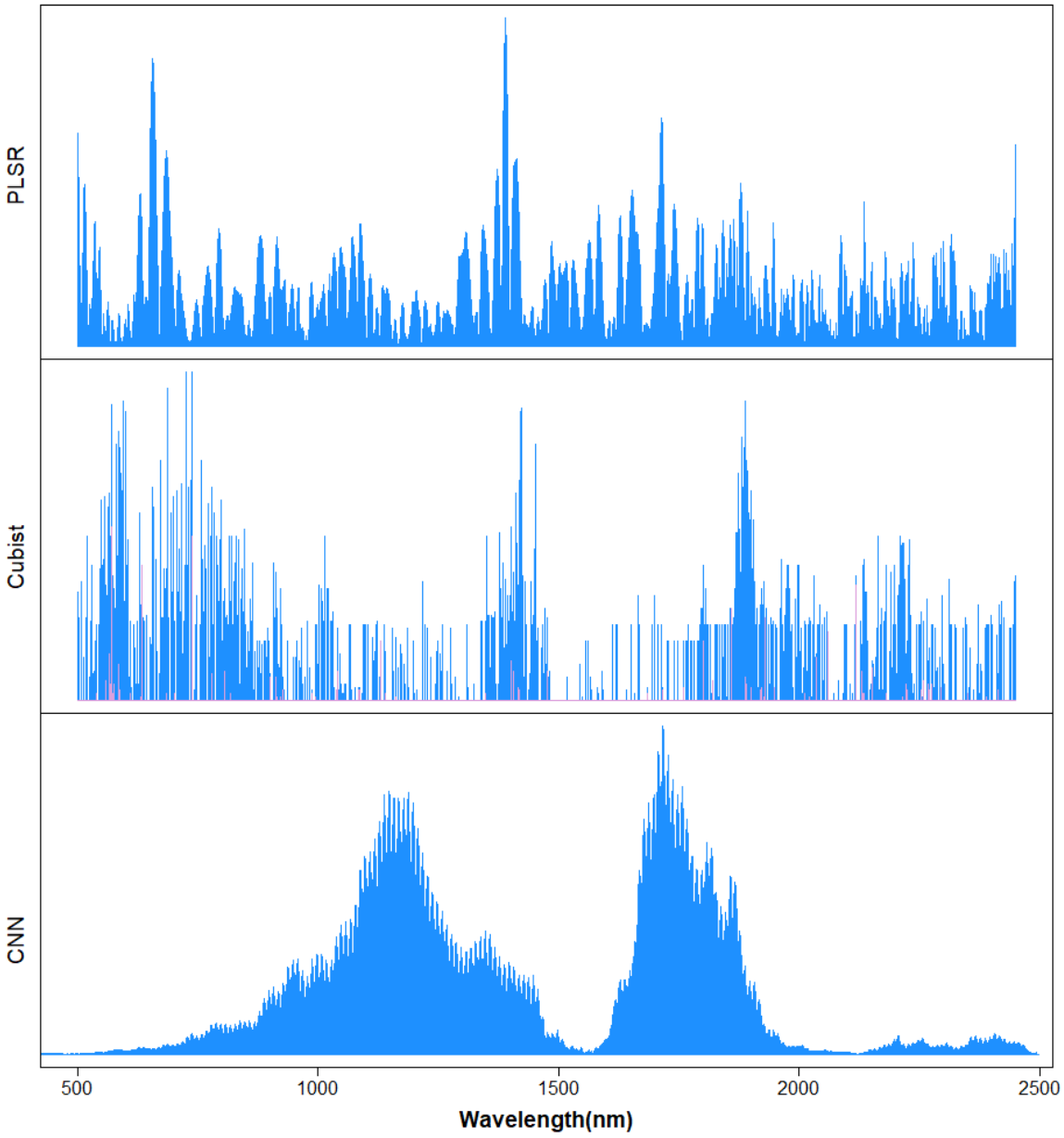

484

485 **Figure 9: Important wavelengths for the prediction of organic carbon (OC) content using Partial Least Squares Regression (PLSR),**

486 **Cubist and Convolutional Neural Network (CNN) model.**

487

Table 1: Descriptive statistics of the soil properties measurements.

	Sand	Silt	Clay	OC	CEC
		g kg^{-1}			$mmol_c$ kg^{-1}
Minimum	50.0	0.0	5.0	1.16	3.4
1st Quartile	644.0	31.0	112.0	3.48	22.9
Median	757.0	57.0	174.7	5.45	32.7
Mean	703.8	69.7	226.5	6.50	37.7
3rd Quartile	839.0	93.5	283.3	8.29	46.3
Maximum	969.0	562.0	840.0	40.02	375.7

Table 2: Architecture of the convolutional neural network.

Type	Shared	Filter size	# Filters	Activation
Convolutional	Yes	20	32	ReLU
Max-pooling	Yes	2	-	-
Convolutional	Yes	20	64	ReLU
Max-pooling	Yes	5	-	-
Convolutional	Yes	20	128	ReLU
Max-pooling	Yes	5	-	-
Convolutional	Yes	20	256	ReLU
Max-pooling	Yes	5	-	-
Dropout (0.4)	Yes	-	-	-
Flatten	Yes	-	-	-
Fully-connected	No	-	100	ReLU
Dropout (0.2)	No	-	-	-
Fully-connected	No	-	1	Linear

*ReLU: rectified linear units

Table 3: Results of model validation for the prediction of various soil attributes using the full calibration dataset.

Model	Properties	Unit	R^2	RMSE	bias	RPIQ
PLSR	Sand	g kg^{-1}	0.79	91.47	2.74	1.29
	Silt		0.47	41.58	-1.78	0.67
	Clay		0.80	73.01	-0.65	0.87
	OC		0.48	2.89	0.02	0.70
	CEC	$mmol_c$ kg^{-1}	0.52	16.77	-0.17	0.57
Cubist	Sand	g kg^{-1}	0.78	89.66	1.28	1.19
	Silt		0.45	38.68	-2.06	0.67
	Clay		0.81	69.65	-0.23	0.92
	OC		0.54	2.80	-0.13	0.70
	CEC	$mmol_c$ kg^{-1}	0.52	17.03	-0.93	0.59
CNN	Sand	g kg^{-1}	0.85	77.28	-0.16	1.52
	Silt		0.58	37.09	-1.74	0.75
	Clay		0.86	60.78	-0.53	1.05
	OC		0.69	2.22	-0.06	0.91
	CEC	$mmol_c$ kg^{-1}	0.68	13.73	-0.76	0.69

OC = organic carbon; CEC = cation exchange capacity